Numerical Investigation of Aerodynamic Analysis on Passenger Vehicle

Cafer Görkem PINAR, İlker COŞAR, Serkan UZUN, Atahan ÇELEBİ, Mehmet Ali ERSOY, Ali PINARBAŞI

***Abstract*—** In this study, it was numerically investigated that a 1:1 scale model of the Renault Clio MK4 SW brand vehicle aerodynamic analysis was performed in the commercial computational fluid dynamics (CFD) package program of ANSYS CFX 2021 R1 under steady, subsonic, and 3-D conditions. The model of vehicle used for the analysis was made independent of the number of mesh elements and the k-epsilon turbulence model was applied during the analysis. Results were interpreted as streamlines, pressure gradient, and turbulent kinetic energy contours around the vehicle at 50 km / h and 100 km / h speeds. In addition, the validity of the analysis was decided by comparing the drag coefficient of the vehicle with the values in the literature. As a result; the pressure gradient contours of the taillight of the Renault Clio MK4 SW vehicle were examined and the behavior of the total force at speeds of 50 km / h and 100 km / h was interpreted.

***Keywords*—** CFD, k-epsilon, aerodynamics, drag coefficient, taillight,

I. Introduction

The vehicle is an extremely important final result for vehicles to reach the underbody of a truck and near the scope of vehicles with complex geometry, as well as for vehicles to complete their projects. Show the vehicle in a way that is displayed in demonstrations of dynamics at a height. [1].

The main developments in vehicle aerodynamics occurred in the early 1980s and today the use of vehicles with low aerodynamic resistance has continued widely [2]. The development of vehicles with low aerodynamic resistance is faster due to the rapid development of technology today, depending on past experiences.[3].

In aerodynamics, not only the reduction of the aerodynamic resistance force is in question, but also the airflow occurring around the vehicle affects the lift force and the position of the center of pressure, which has a significant effect on the vehicle's handling and driving stability. The ground effect caused by the interaction between the underbody of the vehicle and the road has a very small effect on the aerodynamic drag force that opposes the movement of the vehicle but has a significant effect on the life force, which affects the handling of the vehicle.[4].

When designing a vehicle from an aerodynamic point of view, it should be taken into account that the airflow around the vehicle creates water and dirt accumulations on the glass and lamp surfaces of the vehicle. In addition, it is important for the outer body design of the vehicle to reduce the level of wind noise generated around the vehicle due to the movement of the vehicle and to consider the ventilation flows required for cooling the engine, passenger compartment, and brake discs or drums and transmission.[2].

Examination of aerodynamic forces acting on vehicles by experimental and numerical methods has been one of the important issues that have been emphasized from the past to the present. The aerodynamic forces acting on the vehicle in motion are important in terms of affecting the basic parameters of the vehicle such as fuel consumption, exhaust emission values, additional engine power, handling characteristics, and providing road balance under changing road conditions. In studies on vehicle aerodynamics, numerical calculation methods have become more advantageous today because experimental methods take a long time and are costly, measurement devices are expensive, and measurements are difficult on all exterior surfaces of the vehicle.[3].

Because the structure of airflow around a vehicle is highly complex, three-dimensional, and time-dependent, it is not possible to fully model the flow around a vehicle on a computer. In recent years, rapid developments and advances in computer technologies have led to the emergence of a new field of study called Computational Fluid Dynamics (CFD) to realize the approximate solution of many problems in fluid mechanics for which analytical solutions are not possible. In CFD studies, the area to be simulated with the help of a computer and the interactions that occur in this area can be examined in detail. In previous studies, it has been seen that the results obtained using CFD codes are in very good agreement with the experimental results. HAD codes are generally used with commercial package programs. Two or three-dimensional solutions can be made with these codes, as well as the results obtained from the solutions can be shown with graphics and animations. By examining the airflow around the vehicle with CFD, important information about the exterior design of the vehicle can be obtained by analyzing the speed, pressure, aerodynamic force, and moment that are effective on the outer body of the vehicle[3].

Today, after vehicles are generally designed according to body types, necessary corrections for reducing the aerodynamic drag coefficients of the vehicles and other aerodynamic improvements are made by the designers interested in aerodynamics. However, in principle, they pay attention to streamlining vehicle body shapes, as designers are aware that vehicles with low aerodynamic drag coefficients are more attractive.[5]

Djokovic et al. studied the airflow around a passenger car model using a CFD package program. For this study, two- and three-dimensional flow modeling was performed by using the standard k-ε turbulence model. After examining the airflow around the original vehicle model, they changed the angle

İlker COSAR PhD candidate, Yıldız Technical University, Istanbul, Turkey. (e-mail: ilker.cosar@std.yildiz.edu.tr).

between the windshield and the roof of the model vehicle, as well as added wings to the rear of the model vehicle. Then, they compared the analysis results obtained for two different vehicle models. As a result, they determined that the turbulence at the rear of the vehicle model whose exterior design was modified decreases at high cruising speeds, the lift coefficient is positively affected and the driving stability increases. In addition, they found that the wing added to the rear of the model vehicle has double chambers, thus preventing the flow separation at the rear of the vehicle at low cruising speeds, but increasing the aerodynamic resistance force at high cruising speeds.[6].

Barbut and Negrus aimed to reduce the aerodynamic drag coefficient by changing the geometry of the underside of a sedan-type model vehicle by using a HAD package program. For this purpose, they created geometries with different slopes on the underside of the model vehicle and determined that the aerodynamic drag coefficient of the vehicle could be reduced up to 12.7% in this way.[7].

Ahmad et al. used a suitable network structure strategy to accurately calculate the aerodynamic drag coefficient of a passenger vehicle using a CFD package program and aimed to reduce the analysis time by using less computer memory for analysis. For this purpose, three different scales were made for the model vehicle 1:3, 1:4, and 1:5 scale. They found that the analysis time and computer memory used for analysis could be reduced with the smallest scaling and the drag force coefficient could be found with an error of 0.83% based on the experimental data.[8].

Desai et al. carried out numerical and experimental studies to examine the flow around a 1:15 scale model vehicle. A CFD package program was used for numerical studies, and a wind tunnel with cross-sectional dimensions of 300 x 300 x 1000 mm was used for experimental studies. They preferred the Standard K-ε turbulence model for numerical studies. They determined the aerodynamic drag coefficient value as 0.4 in the experimental study and 0.55 in the numerical study. They stated that the high value obtained from the numerical study was due to the simplification of the model tool design used in the study since the computer used for analysis did not have a high-speed processor [9].

In this study; Is it possible to present the CFD analysis of the Renault Clio MK4 SW model vehicle and a development study specifically for the taillight? In this respect to create perspective.

II. MATERIAL AND METOD

A. Fluid Dynamics Equations

Equations of motion for laminar flow of a viscous, incompressible, Newtonian fluid without free surface effects; Continuity equation;

$$\frac{\partial u}{\partial x}+\frac{\partial v}{\partial y}+\frac{\partial w}{\partial z}=0 \quad (1)$$

The generalized form of the continuity equation;

$$\vec{\nabla}\cdot\vec{V}=0 \quad (2)$$

Navier-Stokes equation in the X direction

$$\rho\left(\frac{\partial u}{\partial t}+u\frac{\partial u}{\partial x}+v\frac{\partial u}{\partial y}+w\frac{\partial u}{\partial z}\right)=-\frac{\partial P}{\partial x}+\rho g_x+\mu\left(\frac{\partial^2 u}{\partial x^2}+\frac{\partial^2 u}{\partial y^2}+\frac{\partial^2 u}{\partial z^2}\right) \quad (3)$$

Navier-Stokes equation in the Y direction

$$\rho\left(\frac{\partial v}{\partial t}+u\frac{\partial v}{\partial x}+v\frac{\partial v}{\partial y}+w\frac{\partial v}{\partial z}\right)=-\frac{\partial P}{\partial y}+\rho g_y+\mu\left(\frac{\partial^2 v}{\partial x^2}+\frac{\partial^2 v}{\partial y^2}+\frac{\partial^2 v}{\partial z^2}\right) \quad (4)$$

Navier-Stokes equation in the Z direction

$$\rho\left(\frac{\partial w}{\partial t}+u\frac{\partial w}{\partial x}+v\frac{\partial w}{\partial y}+w\frac{\partial w}{\partial z}\right)=-\frac{\partial P}{\partial z}+\rho g_z+\mu\left(\frac{\partial^2 w}{\partial x^2}+\frac{\partial^2 w}{\partial y^2}+\frac{\partial^2 w}{\partial z^2}\right) \quad (5)$$

The generalized form of the Navier-Stokes equation

$$\left(\vec{V}\cdot\vec{\nabla}\right)\vec{V}=-\frac{1}{\rho}\vec{\nabla}P+\vec{g}+\upsilon\vec{\nabla}^2\vec{V} \quad (6)$$

Reynolds-Averaged Navier-Stokes (RANS) equation for steady, incompressible, and turbulent flow;

$$\left(\vec{V}\cdot\vec{\nabla}\right)\vec{V}=-\frac{1}{\rho}\vec{\nabla}P+\vec{g}+\upsilon\vec{\nabla}^2\vec{V}+\vec{\nabla}.\left(\tau_{ij,türbülans}\right) \quad (7)$$

$\tau_{ij,türbülans}$ term is known as the viscous stress tensor.[10]

$$\tau_{ij,türbülans}=-\begin{bmatrix}\overline{u'^2} & \overline{u'v'} & \overline{u'w'}\\ \overline{u'v'} & \overline{v'^2} & \overline{v'w'}\\ \overline{u'w'} & \overline{v'w'} & \overline{w'^2}\end{bmatrix} \quad (8)$$

B. Computational Fluid Dynamics

There are two basic approaches to the design and analysis of flow engineering systems: experimentation and computation. The former typically requires the construction of models to be evaluated in a wind tunnel or elsewhere, while the latter involves solving differential equations analytically or numerically. With Computational Fluid Dynamics (CFD), details about the flow field such as shear stresses, velocity, pressure distributions, and streamlines of the flow, which cannot be obtained in wind tunnel tests, can be obtained. Thanks to CFD, the product development process can be shortened by reducing the number of tests required for experimental work through carefully controlled parametric studies [11].

While laminar flows can be solved easily with CFD, it is not possible to solve turbulent flows in practice without using turbulence models. There is no general turbulence model that fully resolves turbulent flows, and the turbulent CFD solution is only as good as the turbulence model fits. Despite this limitation, standard turbulence models provide reasonable solutions for most engineering problems in practice [11].

The relations between pressure, viscous and momentum forces that will occur when a fluid flows over a surface are determined by the Navier-Stokes equations. For real flows, these equations can only be solved analytically for simple cases where most of the terms are neglected. In the case of complex, three-dimensional flows, such as flows related to land vehicles, numerical methods must be used to obtain approximate solutions to these equations [11].

The Computational Fluid Dynamics (CFD) approach divides the flow into two regions. The first is the mainstream where viscous effects are neglected, and the second is the boundary layer region where viscous effects become important. It is assumed that the flow in the main flow region is subject to pressure and momentum effects only, and

therefore the flow equations are reduced to a single linear partial differential equation (Laplace equation). The boundary layer region remains very small compared to body dimensions. Therefore, its effect on body shape is negligible. However, when flow separation occurs, the flow cannot be solved by simple analytical equations, as the fluid cannot adhere to the body longer. Initially, numerical solutions are valid for cases where flow separation does not occur. Indirectly, it is possible to determine where the separation will occur and ensure continued validity for any numerical solution. Since the split point changes the velocity, static pressure, and Reynolds number of the air flowing over the body, some corrections are needed to account for it [1].

The computational techniques were reviewed in detail by Ahmed (1998). The first successfully used CFD method was the boundary element method, which is a linear technique in which the body surface of a vehicle is divided into cells. The three-dimensional flow equations are made linear by reconciling the boundary conditions between neighboring cells, and the flow equations are solved to calculate the velocity and pressure at the center of each cell. Nonlinear methods are divided into three categories: Euler methods that neglect friction, Time-averaged viscous (RANS) methods, and discontinuous viscous methods using LES or DNS [1].

Euler's methods take eddies into account but neglect viscosity. The Navier-Stokes equations take into account the relationships between pressure, momentum, and viscous forces in three-dimensional space. These require solving the continuity and conservation of energy equations. Time-averaged (RANS) methods need auxiliary models as they do not take into account the effect of turbulence, and the results are critically dependent on the selection and use of turbulence submodels. Therefore, it calculates the average values of time-averaged pressure and force [1].

LES models recognize that small eddies have a 'universal' character, not dependent on the local flow when calculating large eddies as they are part of the flow. The most complex methods are DNS methods that have no assumptions about turbulence and solve discontinuous Navier-Stokes equations exactly. DNS is capable of giving excellent results with 1-2% error compared to experimental results, but a cell structure divided into million points increases computation time. This computation time requires 24 hours for supercomputers [1].

In this study, the CFX 2021R1 package program, which can solve flow-related equations by using finite volume methods, is used to calculate the flow area numerically. In the analysis made with the CFX package program, the sensitivity of the network structure in the region where the flow event occurs depends on the characteristics of the computer used. The CFX package program uses the computer memory according to the size of the problem while performing the analysis. The extent of the problem is the state of the network structure, the number of cells, and the laminar or lateral flow of the flow.

C.Geometry

The vehicle model used during the simulation was modeled in the NX CAD program and transferred to the geometry part of the ANSYS CFX package program. As can be seen in the Fig. 1, while designing the vehicle model in the NX program, some parts of the vehicle's wheels, such as rim compartments, front cooling channels, and side mirrors, were ignored due to the inadequacy of the computer capacity used for simulation. Necessary improvements have been made for the body of the vehicle model in the geometry part of the CFX package program.

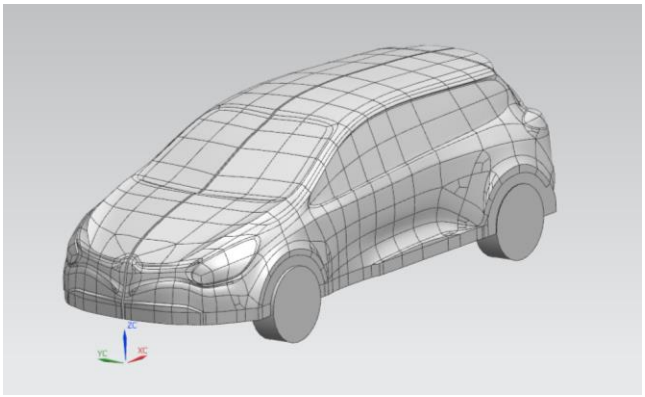


Fig. 1 Model Geometry

D.Domain

The compute domain can be designed with a negligible block rate. The dimensions of the domain are determined to be proportional to the length of the car placed in it, as seen in the figure. After the vehicle was placed in the domain, it was removed from the domain and the vehicle body was created to be hollow in the domain.

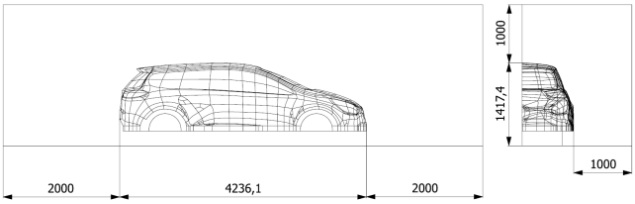


Fig. 2 Analysis Model

In the thesis study, the model of the Renault Clio MK4 (Mark4) SW (Station Wagon) brand vehicle with a scale of 1:1 was used. Half model is used in vehicle geometry. (Fig. 2)

E. Mesh Model

Analysis from the 3D model CAD input with the tool before. While creating the model, Renault S.A company is guided by the vehicle in its own published catalog. The CAD model has been converted to a step extension to make it compatible with the Ansys CFX representation where the analysis is performed. For meshing, the Ansys SpaceClaim fit model was engulfed in a fluid volume and transition corrections were made.

The data obtained from the meshing process are given in the Table I below.

TABLE I
NODES AND NUMBER OF ELEMENTS

	Nodes	Elements
1. Mesh Model	1118321	3697974
2. Mesh Model	1414906	4841983
3. Mesh Model	1787327	6134347

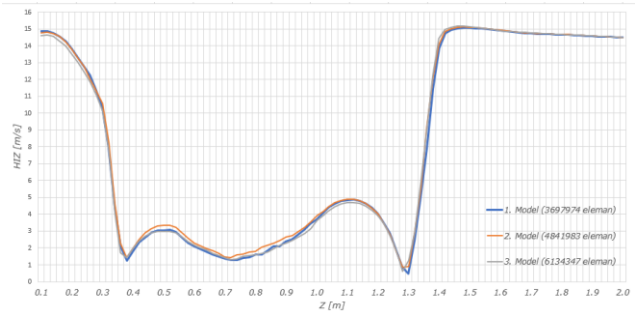


Fig. 3 Mesh Data

Looking at the graph in Fig. 3, when the data are compared according to the mesh number of the velocity gradients formed at the rear of the vehicle, it is understood that the mesh density used in the analysis is made independent of the mesh density with a low error.

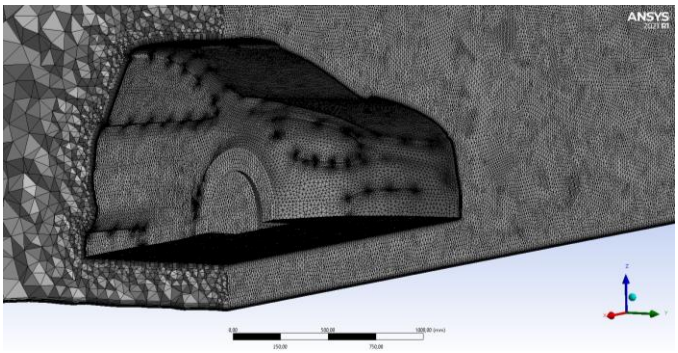


Fig. 4 Meshed State of Analysis Geometry

F.Boundary Conditions

The boundary conditions used in the analysis process are given in Table II.

TABLE II
LIMIT CONDITIONS USED

Type	Region	Motion Status
Inlet	Region perpendicular to the front of the vehicle	50[km/h] & 100[km/h]
Opening	Aperture Pressure and Direction	0 [Pa]
Wall	Car Floor	u=50 km/h & 100 km/h
Wall	Car & Car Taillight	motionless
Symmetry	The symmetry axis of the vehicle	motionless

Since the k-epsilon turbulence model is used in aerodynamic analysis studies in the literature, the k-epsilon turbulence model was used again in this study.

In the analysis, the speed of the airflow coming to the surface of the vehicle as the entrance boundary condition was taken as 50 km/h in the first analysis and 100 km/h in the second analysis. Since the sonic speed was determined by the Mach number, the speed of the air under the determined conditions remained below the speed of sound. For this reason, the flow regime was considered subsonic. The temperature of the fluidized air at continuous ambient conditions was accepted as 25°C, which is accepted under normal conditions. Also, mass and momentum were accepted as normal velocities. Turbulence acceptance was taken as Eddy Viscosity Ratio and Normal Density.

The opening boundary condition was chosen as the parts of the flow volume that are outside the inlet and symmetry axis, far enough from the geometry of the vehicle. In addition, since we work in stagnant conditions, the flow regime is considered subsonic. The direction of Mass and Momentum was determined as 0 Pa in the form of opening pressure and direction. Turbulence acceptance was taken as Eddy Viscosity Ratio and Normal Density.

The axis of symmetry was chosen as the surface where the cross-section of the vehicle is. The reason for this is that it calculates using half of the tools in the analysis and reflects the whole in the results.

The boundary condition selected as wall is all surfaces belonging to the body of the vehicle. The reason for this can be shown by examining the airflow that will occur around the vehicle. Airflow will not pass through the surfaces selected as walls and will move from its surface.

G. Validation

The c_D creep coefficient in this study was obtained because of the analysis as 0.3544 for 50 km/h speed. As seen in the graph below, it is seen that it converges to this value according to the number of iterations. (Fig. 5 and Fig. 6)

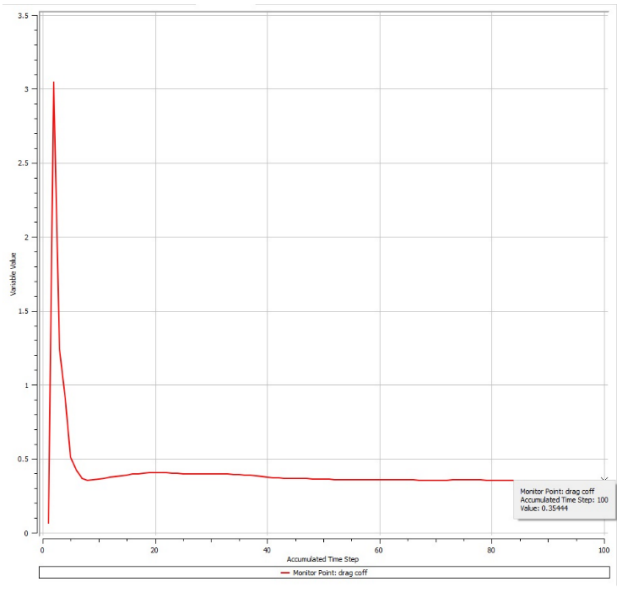


Fig. 5 c_D coefficient at 50 km/h

In addition, when the analyzes are repeated at 100 km/h, it is seen that the cd coefficient converges to the value of 3.5618 and the number of iterations. It is understood that the 0.35

creep coefficient value is reasonable for the passenger car c_D coefficient obtained in the literature and the analysis is valid.

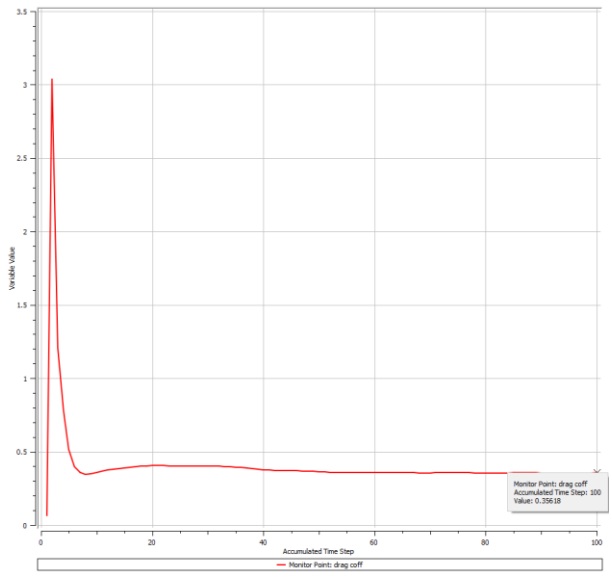


Fig. 6 c_D coefficient at 100 km/h

We can also do this calculation with the formulation. [10]

$$c_D = \frac{2F}{U^2 \cdot \rho \cdot A} \tag{9}$$

Here we need the front projection area of the vehicle to be used in the formulation. We obtained the area as data from the CAD model of our vehicle. Since we are using a half-section, the cross-sectional area of the full vehicle model must be divided into two. From here, A= 0.925 m^2 is determined. Its formula allows us to find the drag coefficient c_D. If we write the total force (Table III and Table IV), area, and air density on the vehicle model into the equation, we get c_D =0.35444 for 50 km/h.

TABLE III
FORCES ON THE VEHICLE AT 50 KM/H

Location	Type	X (Drag Force) [N]	Z (Lift Force) [N]
Car	Pressure Force	33.826	-8.1046
	Viscous Force	3.6516	0.35178
	Total Force	37.477	-7.7529

TABLE IV
FORCES ON THE VEHICLE AT 100 KM/H

Location	Type	X (Drag Force) [N]	Z (Lift Force) [N]
Car	Pressure Force	137.56	-36.048
	Viscous Force	13.097	1.1899
	Total Force	150.66	-34.858

III. RESULTS

The result of the velocity distribution of the air around the vehicle from the CFD model is shown in Figure 7. As seen in the figure, a high speed zone has formed on the hood and roof of the vehicle. In addition, a low velocity region was formed as a result of the flow separation in the region between the hood and the ceiling. A low speed region has formed because the air flow has slowed or stopped on the front nose of the vehicle. As the flow separation occurred at the rear of the vehicle, a lower velocity flow region was formed and thus a trailing area was formed. Under the vehicle, a high speed zone has occurred due to the flow restriction.

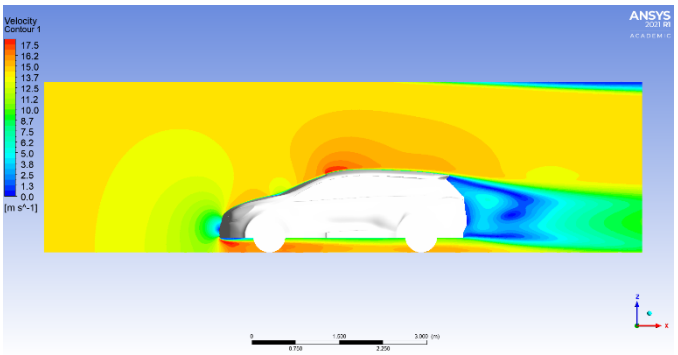


Fig. 7 Speed contour 50 km/h

The streamlines and pressure gradients we obtained when we performed our analysis are given below.

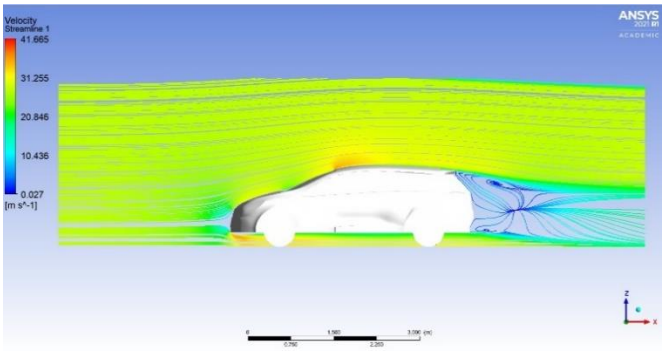


Fig. 8 100km/h streamline

As seen in the Fig. 8, it is shown how the streamlines formed on the vehicle along the mid-plane of the vehicle change depending on the surface geometry. Streamlines are separated from the surface as a high-pressure zone is formed in the front of the vehicle. Since high pressure was created in the region between the hood and the windshield, the streamlines could not follow the surface geometry here, and as the air velocity increased in the next region, the air pressure decreased, and this resulted in the air following the surface geometry again. At the back, as the air molecules could not adhere to the surface due to the geometry of the surface, flow separation occurred again, and this caused the streamlines to not follow the surface geometry.

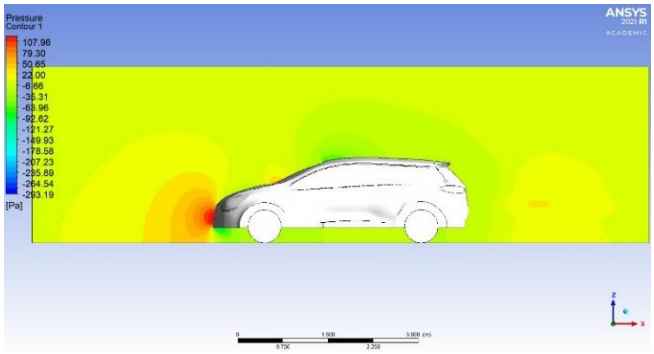


Fig. 9 Pressure contours at 50 km/h

As seen in Fig 9, the static pressure distributions formed on all surfaces of the body of the vehicle are shown. As can be seen from the figure, high-pressure zones have formed at the front of the wheels due to the flow stop. Due to the flow stop on the front nose, the air tried to escape to the sides, and therefore there was a decrease in the static pressure of the air on the sides. As the air passed over the hood, its pressure decreased, but when it reached the windshield, there was a rapid increase in pressure. The air, which had high pressure at the beginning of the windshield, accelerated as it passed over the windshield, and therefore, the pressure decreased to negative levels. After this pressure drop, it is understood from the figure that the static pressure of the air decreases further at the junction of the windshield and the ceiling and continues along with the ceiling. Therefore, an upward lifting effect was created on the vehicle along the roof of the vehicle.

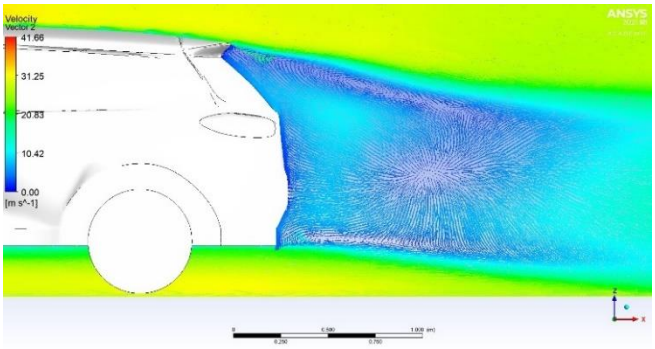


Fig. 10 Speed vectors at 100 km/h

As can be seen in the Fig. 10, the direction and intensity of the flow motion occurring along the midplane of the vehicle are shown together with the velocity vectors. It is observed that eddies are formed in the regions where flow separation occurs. Since the turbulence intensity is higher at the rear of the vehicle, more eddy movements have occurred compared to other regions. (Fig. 11) The eddy movements formed behind the vehicle created a trace area as seen in the figure. In this region, the contact of the air with the body of the vehicle has weakened and the surface friction resistance has decreased.

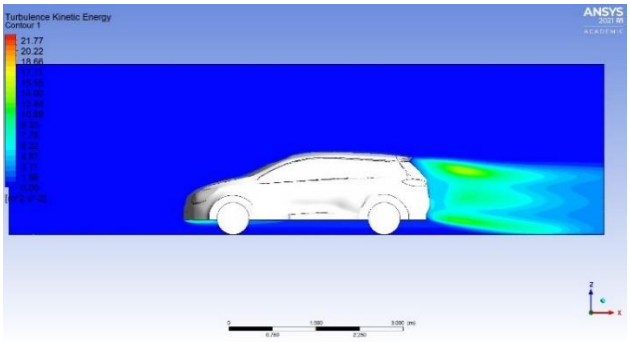


Fig. 11 Turbulent kinetic energy at 50 km

The Fig. 12 shows the contour diagram of the drag force in the vehicle.

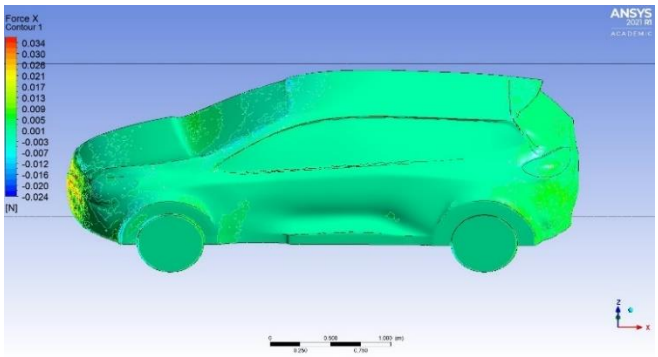


Fig. 12 Force on the vehicle at 50 km/h

In the Fig. 13, it is seen in the contour diagram of the drag force on the taillight in the vehicle. The figure shows that critical forces have accumulated in the center of the taillight.

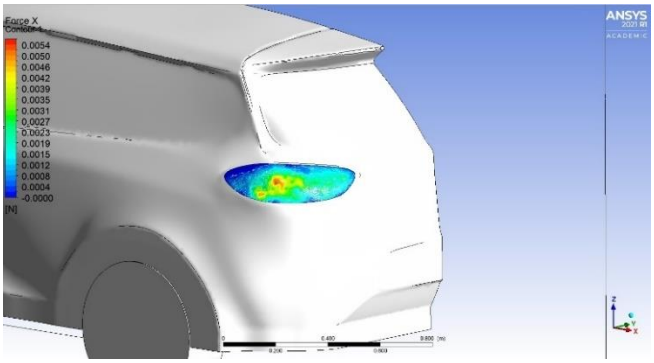


Fig 13 Forces on the taillight at 50 km/h

IV. CONCLUSION

In this study, the drag coefficient, which is directly related to the aerodynamic efficiency of a 1:1 scale vehicle model, was calculated by using the CFX package program. The analyzes were repeated at different speeds and as a result, although the drag coefficient in the literature was caught, it was also observed that it increased in direct proportion to the speed. This showed that the analysis was successful. Then, the flow events around and above the vehicle model, which is the output of the study, were visually examined.

The results of the study are as follows.

It has been determined that the data in the numerical study

are in harmony with the literature. In addition, it is understood from this situation that the mesh model used in the study and the boundary conditions used in the study are accurate. However, it should be accepted that the drag coefficient obtained due to simplifications and omissions on the model converged to the actual results at a certain error rate. However, in the study, it can be interpreted in which regions improvement can be made on the Solid model, thanks to the aerodynamic analysis.

In our study, it has been argued that the improvement on the taillight may have aerodynamic effects, apart from the effect on the exterior aesthetic design of the vehicle.

The materials and manufacturing methods used in the taillight bodies can provide flexibility in design. It can therefore be a simple and effective way to improve a vehicle's aerodynamics.

ACKNOWLEDGMENT

This research was conducted by Pleksan Industry and Trade inc. was sponsored.

REFERENCES

[1] Stone, R., Ball, J.K., 2004. Automotive Engineering Fundamentals, Warrendale,435-454.

[2] Gillespie, D.T., 1992. Fundamentals of Vehicle Dynamics, Warrendale, 85– 98.

[3] Hucho, W.H., Savran G., 1993. Aerodynamics of Road Vehicles, Annu.Rev. Fluid

[4] Heisler, H., 2002. Advanced Vehicle Technology, Butterworth-Heinemann, Oxford,584-617.

[5] Julian, H. S., 2002. An Introduction to Modern Vehicle Design, Butterworth-Heinemann, Oxford, 111-112.

[6] Damjanovic, D., Kozak, D., Zivic, M., Ivandic, Z., Baskaric, T., 2011. CFD Analysis of Concept Car In Order to Improve Aerodynamics, Járműipari innováció, 01/02,108-115.

[7] Barbut, D., Negrus, E.M., 2011. CFD analysis for road vehicles- case study, Incas Bulletin, 3, 15-22.

[8] N. E. Ahmad, E. Abo-Serie, A. Gaylard, 2010. Mesh optimization for ground vehicle aerodynamics, CFD Letters, 2, 54-65.

[9] Desai, M., Channiwala, S.A., Nagarsheth, H.J., 2003. Experimental and Computational Aerodynamic Investigations of a Car, Wseas Transactions on Fluid Mechanics, 3, 359-367.

[10] Çengel, Y.A. and Cimbala, J.M. 2006. Fluid Mechanics: Fundamentals and Applications. 992 pp. McGraw-Hill Higher Education, Boston

[11] Katz, J., 2006. Aerodynamics of Race Cars, Annual Reviews Fluid Mechanics, 53-57.